

FLEXURAL FATIGUE BEHAVIOUR OF TEXTILE-REINFORCED CONCRETE PANELS

KEERTHANA KIRUPAKARAN^{*}, NERSWN BASUMATARY[†] ROSHINI RAMANATHAN[‡]

^{*+‡}Department of Civil Engineering

^{*+‡}Indian Institute of Technology Madras, Chennai, India

^{*}e-mail: keerthanak@civil.iitm.ac.in

[†]e-mail: nerswnb.civil@gmail.com

[‡]e-mail: roshiniramanathan14@gmail.com

Keywords: Textile Reinforced Concrete, Fatigue, Stiffness, Monotonic, Crack width

Abstract: In this research, the flexural fatigue performance of Textile Reinforced Concrete (TRC) panels is experimentally evaluated. TRC panels made of four layers of E-glass textile fibres are prepared and tested under a three-point bending configuration in conjunction with the Digital Image Correlation (DIC) technique. The load-deflection response, stiffness degradation, and crack propagation are evaluated to understand the fatigue damage progression in TRC panels, and a comparison is drawn between its monotonic and fatigue behaviour. From the analysis, it is realized that the fatigue strength of TRC panels could be considered until when fatigue deflection value reaches 70 % of the deflection value corresponding to the strain-hardening peak load of monotonic response. The DIC results reveal that the failure of TRC specimen due to fatigue loading takes place at a significantly lower crack width compared to the monotonic loading. Further, the TRC panels under fatigue fail with sufficient warning through visible large deformation, unlike plain concrete.

1 INTRODUCTION

Textile Reinforced Concrete (TRC) is a high-performance cement-fiber composite material that has a huge potential to be used as facades in high-rise buildings. TRC has a high bearing capacity and ductility as compared to plain concrete and it can be used to make thin and lightweight structures [1-3]. The use of TRC as facades has two main advantages: Firstly, unlike glass facades which fail in a brittle manner, they show high ductility before failure. Secondly, in tropical countries like India, TRC facades can drastically reduce operational energy consumption compared to buildings made of glass facades which induce the greenhouse effect [4-5]. Furthermore, it is reported that the use of glass facades in skyscrapers poses a significant risk to birds, as they may not recognize the transparent surfaces

due to highly reflective glass facades [6].

Currently, the use of TRC facades in low-rise buildings is gaining momentum and they can be a potential substitute for facades in high-rise buildings as well [7-10]. Even though TRC facades are not transparent like glass facades, they can be aesthetically engineered with or without glass components. In high-rise buildings, variable wind velocities are the prominent loads and induce fatigue failure [11]. Further, during severe cyclones, ductile TRC facades can perform better compared to glass facades which have failed catastrophically in such extreme scenarios [12]. While we can foresee the potential of TRC facades in high-rise buildings, there are several gaps in the fundamental understanding of the behaviour of TRC façade panels under fatigue loading and it is scarcely explored in the literature.

Numerous researchers have shown interest in investigating the mechanical response of TRC composites. The behaviour of TRC is influenced by several key factors, including the type of textile reinforcement used, its mechanical properties, and the volume of reinforcement composite, which is determined by the number of reinforcement layers and the surface area over which it is distributed [13-15]. The behaviour of TRC under static flexural loading conditions can be divided into two zones. In zone I, the composite action of concrete matrix and textile reinforcement plays a dominant role and the cracking of concrete takes place. In zone II, the load is transferred from the concrete matrix to textile reinforcement and the strain hardening or under-reinforced behaviour is observed depending on the volume fraction of textile reinforcement [16]. Zargaran et al. [16] performed a four-point bending and reported that the performance of samples with the strain-hardening behaviour is improved by decreasing mesh size and greater yarn tex in reinforced composites with the same reinforcement ratio. Hegger et al. [17] examined the flexural behaviour of TRC reinforced with textiles made of carbon and alkali-resistant (AR) glass fibres and studied the effect of the reinforcement ratio on the ultimate stress, crack spacing, and elongation in the tension zone of TRC. Halvaei et al. [18] studied the behaviour of TRC under a four-point bending test and reported a reduction in the textile mesh size from 20 to 2 mm led to an increase in the sample's flexural load and toughness of more than 380% and 820%, respectively. Mesticou et al. [19] investigated the behaviour subjected to fatigue loads equivalent to 60% and 80% of the rupture load and reported residual behaviour of TRC did not exhibit any deterioration following the fatigue cycles. Wagner et al. [20], studied the bond fatigue of TRC under uniaxial tension with epoxy-impregnated carbon textiles that the anchorage length plays a crucial role in determining the bond strength. Similarly, Munck et al. [21] examined the fatigue behaviour of sandwich beams under a four-point bending test and reported that the original rigidity is decreased because of crack

formation. Although few researchers studied the fatigue behaviour of TRC under tensile loading, investigation under flexural fatigue loading remains a relatively under-explored subject. Therefore, due to the absence of standards/guidelines available for designing/testing TRC facades, there is a lack of confidence in its wider application though it shows potential for better performance in terms of bearing capacity, bending and ductility. In this research, the flexural fatigue performance of TRC panels is evaluated through an experimental program. TRC panels made of four layers of E-glass textile fibres are prepared and tested under a three-point bending configuration. The load-deflection response, stiffness degradation, and crack propagation are evaluated to understand the fatigue damage progression in TRC panels. Mechanical tests are performed in conjunction with the Digital Image Correlation (DIC) technique to characterize mechanical performance and fracture behaviour. Finally, a comparison is drawn between its monotonic and fatigue behaviour.

EXPERIMENTAL PROGRAM

2.1 TRC panel specimen preparation

2.1.1 Concrete mix

The matrix composition of the concrete mixture consists of a combination of Ordinary Portland Cement (OPC), fly ash, and micro silica as shown in Table 1. A Poly Carboxylate Ether (PCE) superplasticizer is added to the mixture at a rate of 0.15% by weight of the binder to improve the characteristics. The maximum aggregate size is limited to 1.2 mm to facilitate smooth aggregate penetration through the textile grid. As a result, high-strength concrete with a 28th-day compressive strength of 50 MPa is produced, as shown. The mechanical properties of the concrete mix are shown in Table 2.

2.1.2 Textile reinforcement

The mortar matrix contains a leno weave textile reinforcement fabricated from E-glass

rovings as shown in Figure 1. The schematic of the leno weave is shown in Figure 2. According to the manufacturer, the textile possesses a nominal tensile strength of 1650 MPa and a modulus of elasticity of 70 GPa. Table 3 provides detailed information on the properties of this textile reinforcement, including its mesh opening size of 16×16 mm. TRC panels of dimension $200 \times 400 \times 35$ mm are prepared with 4 layers of E-glass textile fabric at a 7 mm centre-to-centre distance from each other along the thickness.

Table 1: Concrete mix details

Materials	Values
Cement(kg/m ³)	: 583
Fly ash (kg/m ³)	: 208
Silica fume (kg/m ³)	: 42
Quartz sand (kg/m ³)	: 595
Quartz powder (kg/m ³)	: 357
Water/binder	: 0.4
Maximum size of aggregate (mm)	: 1.2
PCE superplasticizer (%)	: 0.15

Table 2: Mechanical properties of concrete

28-day compressive strength	: 50 MPa
28-day tensile strength	: 4.5 MPa
28-day flexural strength	: 6.9 MPa
Modulus of Elasticity	: 30 GPa
Age of the specimen	: 1.5 Years

Table 3: Properties of textile fibre

Type of fibre	: E-glass
No. of textile layer	: 4
Diameter of Textile	: 0.9 mm^2
Type of weaving	: Leno weave
Grid size	: $16 \times 16 \text{ mm}$
Volume fraction of fibre	: 0.91%
Modulus of elasticity	: 70 GPa

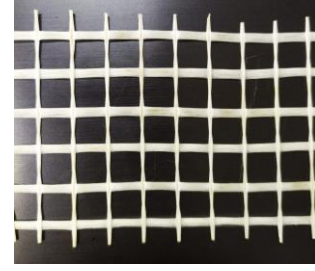


Figure 1: Leno weave E-glass fibre

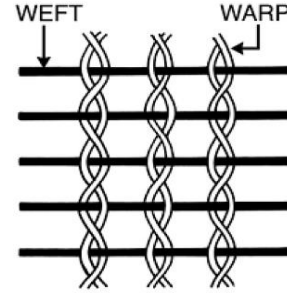


Figure 2: Schematic of Leno weave textile fibre [22]

2.2 Experimental set-up and loading parameters

2.2.1 Three-point bending test

The flexural monotonic and fatigue tests on TRC panels are performed on a servo-hydraulic machine of capacity 100 kN. TRC panels of $200 \times 400 \times 35$ mm size with a span length of 150 mm is tested under a three-point bending configuration as shown in Figure 4. The load-point vertical displacement is measured using Linear Variable Differential Transformer (LVDT) mounted at the mid-span below the specimen. TRC specimens are initially tested under monotonic loading to obtain the peak load and first crack load. Then the specimens are tested under variable amplitude fatigue loading composed of the sinusoidal waveform of 1 hertz frequency. The fatigue loading pattern is depicted in Figure 3. A fatigue loading cycle composed of a minimum load amplitude of 0.2 kN is maintained to ensure contact between the loading device and the specimen. The maximum load amplitude is increased after every 1000 cycles in the steps of 0.25 kN starting from 1.5 kN to 3 kN. The fatigue load amplitude of the last load step is continued until failure. The maximum

amplitude of 3 kN was chosen such that it is 75% of the monotonic peak load. The data such as time, load, actuator displacement, and LVDT are simultaneously acquired through a data acquisition system. To understand the fracture mechanisms in TRC panels under fatigue, the Digital Image Correlation (DIC) technique is used which is described in the following section.

2.2.2 Digital Image Correlation (DIC) set-up

Digital Image Correlation (DIC) is an optical measurement technique that enables non-contact monitoring of surface displacement and strain in a deforming object. Figure 5 depicts the DIC setup. This method involves applying a black-and-white speckle pattern to the specimen's surface and capturing consecutive digital images as the object undergoes deformation. Using a correlation algorithm, the displacements and stresses on the specimen's surface are analysed by tracking the movement of pixels in the digital images of the deforming specimen. In this experiment, a black and white

matte finish spray is evenly applied to the beam specimens to create the necessary speckle pattern. A 12.3-megapixel resolution camera is employed to capture digital photos. The camera is firmly attached to a tripod support and set up so that its axis is parallel to the plane of the deforming specimen. The pictures are taken at a rate of 10 frames per second. Subsequently, DIC analysis is performed on the images using Istra 4D which is an image processing software [23].

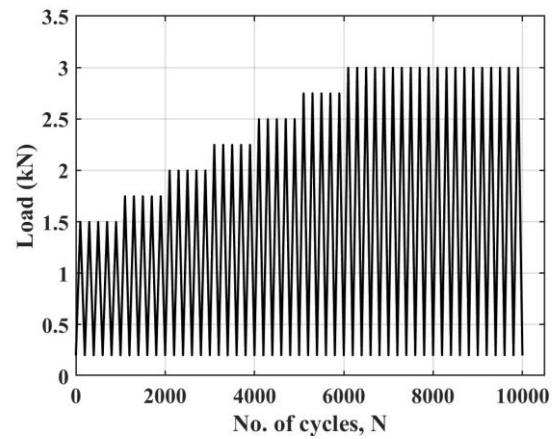


Figure 3: Variable amplitude loading

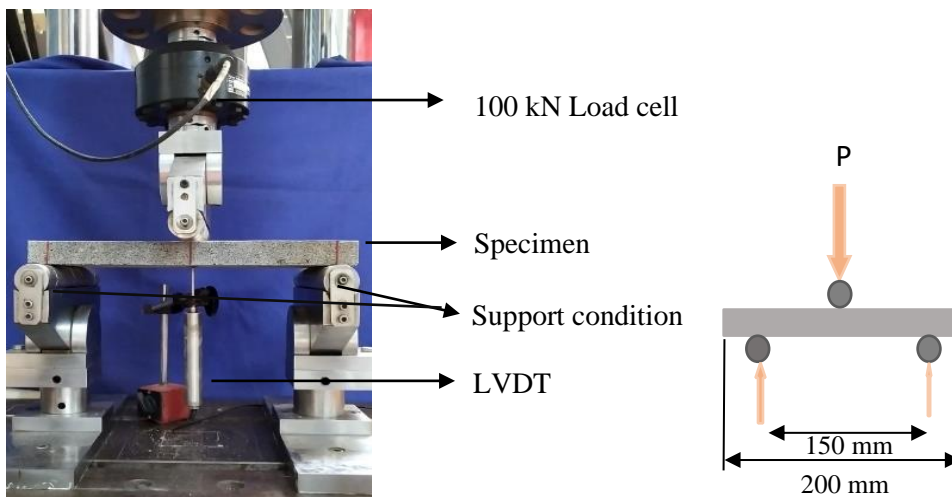


Figure 4: Experimental set-up for three-point bending test

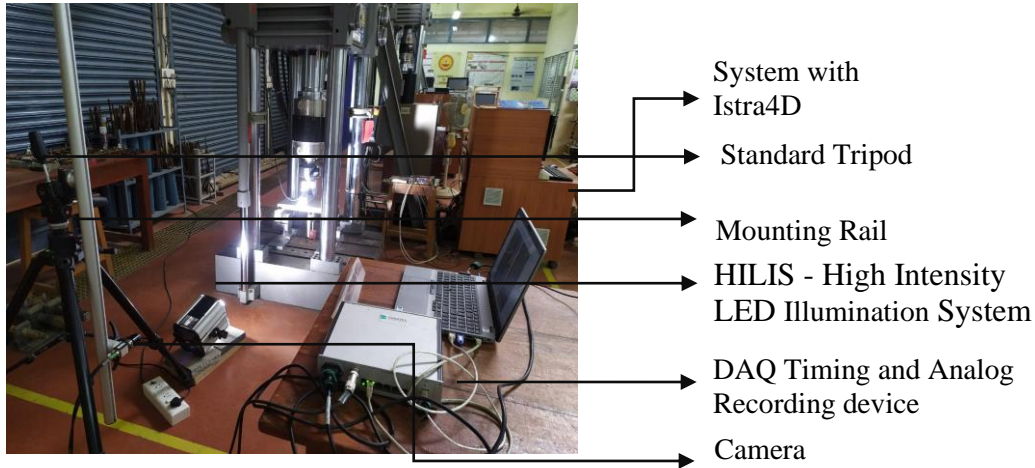


Figure 5: Experimental set-up for Digital Image correlation (DIC)

3 EXPERIMENTAL TEST RESULTS

3.1 Mechanical test results

3.1.1 Monotonic test results

A flexural test under a three-point bending configuration was performed on a specimen of size $200 \times 400 \times 35$ mm at a loading rate of 1 mm/min. The results of the load-deflection response are depicted in Figure 6. Four zones are marked in the figure as Zone 1 (O-A), Zone 2 (A-B), Zone 3 (B-C), and Zone 4 (C-D). Zone 1 corresponds to an elastic zone with point A indicating the first crack load in the concrete mortar matrix. Beyond point A, microcracks in concrete occur and a sudden drop is observed till point B. Between points B and C, strain hardening occurs due to the composite action of TRC. Three specimens are tested under monotonic loading and the average peak load of 4 kN with a standard deviation of 0.62 kN is obtained. This average peak load is taken as the reference for selecting the maximum amplitude for the fatigue step loading as discussed earlier in section 2.2.1.

3.1.2 Fatigue test results

Flexural fatigue tests are performed on three TRC specimens and their fatigue failure cycles are shown in Table 4. The load-deflection response of three TRC specimens subjected to fatigue loading is shown in Figure 7 (a-c). The

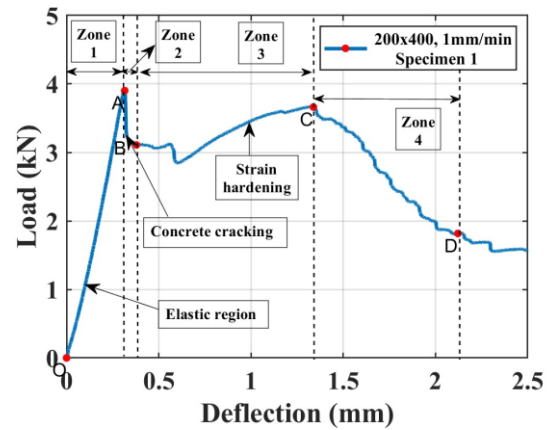


Figure 6: Load-deflection curve of TRC under monotonic loading

typical behaviour observed in all the specimens is that the slope of the load-deflection curve at every load cycle gradually decreases with the increase in fatigue load cycles. The decrease in slope becomes more prominent after about 30% of the fatigue cycle in two specimens (Figure 7(a) and (b)) and for the last specimen slope decrease is prominent after about 15% of fatigue life. A Point M is marked and a line is drawn through point M in all the figures such that beyond this point non-linear behaviour sets in. The deflection value is approximately 1.2 mm corresponding to point M in two of the specimens, and the deflection value is 0.35 mm at M for the third specimen which is considered an outlier. For the first two specimens, point M lies approximately at 30% for fatigue life. TRC specimen undergoes non-linear behaviour due

to the cracking of the concrete matrix, and load is transferred to the textile reinforcement. At later stages of fatigue life, a sharp decrease in slope accompanied by a larger area under the hysteresis loop is observed. This observation is attributed to the unstable fatigue crack propagation. However, unlike plain concrete, the TRC panel specimen failed after sufficient warning. At the time of failure, textile reinforcement elongated and some of them got ruptured while a few of them were still intact holding the specimen from falling.

The degradation of stiffness under fatigue load cycles is shown in Figure 8 (a) and (b) for two specimens. The stiffness is calculated as the slope of the unloading curve of fatigue load cycles. A huge scatter is observed in stiffness values and this scatter is large until 50% of fatigue life. This observation can be attributed to the composite nature of TRC. The

degradation of the interface zone due to micro-cracking in the concrete matrix and redistribution of load to textile reinforcement with higher stiffness during the loading and unloading phase of fatigue cycles can be the reason for the undulating nature of stiffness values. However, the generic decreasing trend in stiffness with fatigue loading cycles is observed in the figures as depicted by the solid line.

Table 4: Number of cycles up to failure

Specimen No.	No. of fatigue cycles up to failure	Standard deviation
S1	11682	3510
S2	12259	
S3	4540	

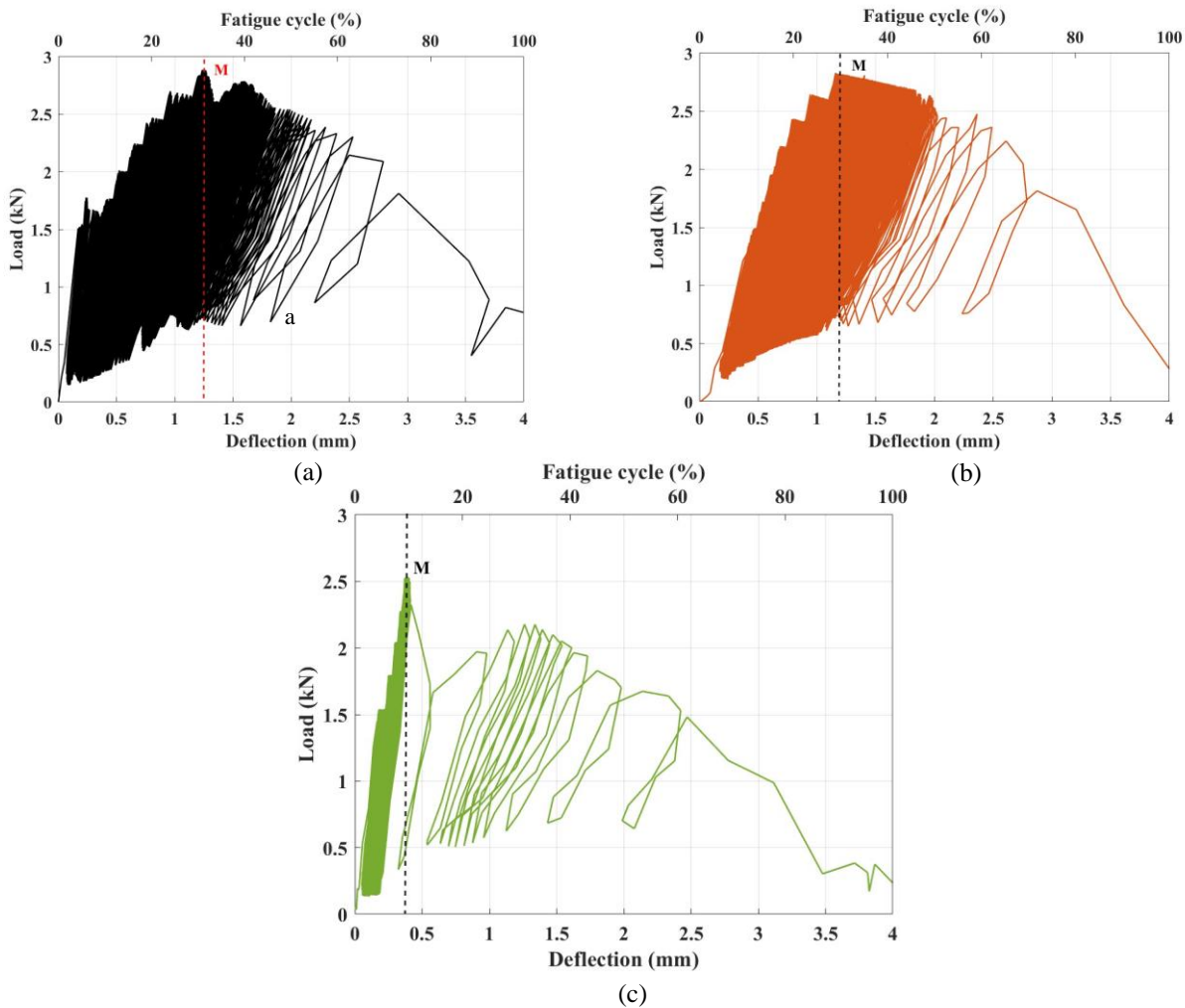


Figure 7: Load-deflection curve of TRC panel under fatigue loading for (a) specimen 1, (b) specimen 2 and (c) specimen 3

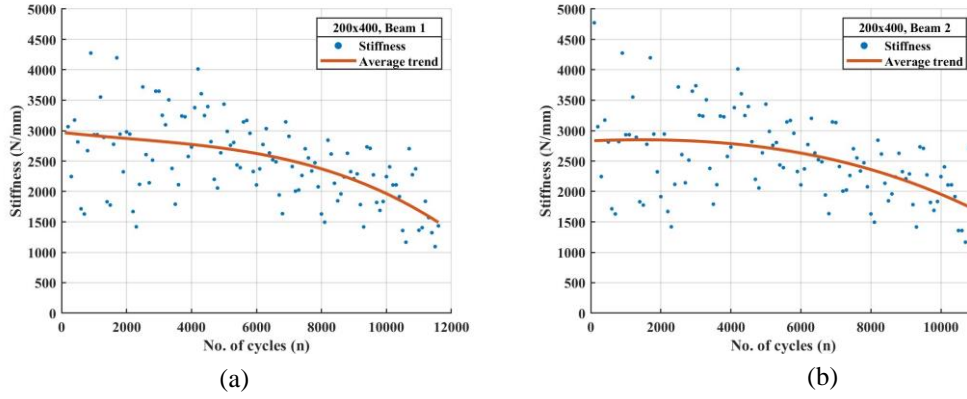


Figure 8: Stiffness versus number of cycles (a) specimen 1 and (b) specimen 2

To understand and correlate the performance of TRC under fatigue with its monotonic behaviour, the load-deflection response of TRC panels under flexural fatigue and monotonic loading are superimposed as shown in Figure 9. The fatigue load and deflection values corresponding to points A, B, C, and D of the monotonic curve are shown in Table 5. The following observations are made from Figure 9:

1. Comparing the initial stiffness of TRC under monotonic loading and the stiffness of TRC under fatigue loading corresponding to deflection at B, not much variation is observed. This indicates that until deflection at point B, the TRC behaviour under fatigue remains elastic. Hence, the monotonic deflection value corresponding to point B can be considered as the critical deflection value for fatigue such that beyond this deflection value TRC under fatigue will undergo non-linear deformation.
2. Between points B and C, strain hardening is observed under monotonic due to the effective transfer of load between concrete matrix and textile reinforcement. The fatigue performance of TRC between points B and C also improves. This improvement can be observed in Figure 8 as well, which shows the scatter of stiffness values with the fatigue cycles. The generic stiffness trend shows a plateau and only in the later stages of fatigue life a significant decrease in stiffness is observed.
3. Despite the non-linearity in the material, TRC performance under fatigue between the deflection points B and C is good as it has

- sufficient load carrying capacity which is evident from the stiffness curves.
4. Deflection at Point M, defined earlier for fatigue response lies closer to deflection at point C of the monotonic load response. From these observations, 70% of the deflection value corresponding to point C in the monotonic load-deflection curve can be used as a limiting deflection point for the design of the TRC panel for fatigue strength. In other words, the fatigue strength of TRC panels should be considered only until the 70 % deflection value corresponding to point C in a monotonic curve.
5. Beyond point M, unstable crack propagation under fatigue is observed. Unlike plain concrete, TRC panels show sufficient warning through visible large deformation before failure. This is an important feature of TRC for its potential application as facades in high-rise buildings.

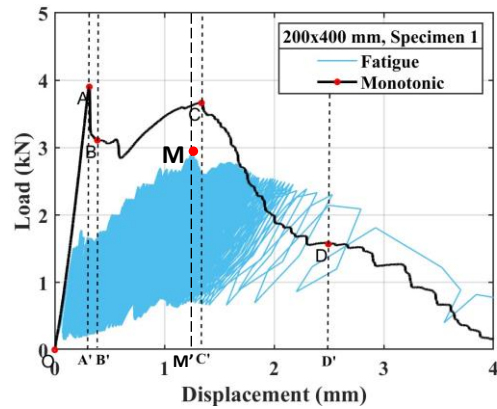


Figure 9: Comparison of load-deflection curve under monotonic and fatigue loading

Table 5: Comparison of displacement values at monotonic and fatigue loading

Specimen	Displacement values under monotonic at points			Displacement values under fatigue corresponding to monotonic curve	
	A' (mm)	C' (mm)	D' (mm)	A' (mm)	D' (mm)
1	0.37	0.79	3.2	1.23	2.53
2	0.37	0.82	4.6	1.15	2.48
3	0.25	0.91	1.8	0.38	2.49

3.2 Interpretation of DIC results

Digital Image Correlation (DIC) technique is used to analyze the crack pattern and its propagation with fatigue cycles. The surface strain contour plot obtained from DIC analysis is shown in Figure 10 for the TRC panel at fatigue failure. Three cracks had initiated from the tension side of the beam and only the mid crack propagated until the entire depth of the specimen. The multiple cracking is attributed to the role of the textile reinforcement.

During the initial stages of fatigue life, the surface cracks were not prominent, hence no crack length is observed from DIC analysis. Only in the later stages, surface cracks were prominently visible in DIC analysis. The crack grows at a very slow rate during the initial stages of fatigue loading. Though the crack is not reflected on the specimen surface, the scatter seen in the stiffness degradation curve (Figure 8) is an indication of crack growth. With an increasing number of load cycles and load amplitude, the crack propagates in a stable manner until deflection corresponding to point M. Beyond point M, non-linearity sets in due to redistribution of load and crack-bridging effect of textile reinforcement. The crack pattern on the top face of the TRC specimen tested under monotonic and fatigue loading are shown in Figures 11 and 12 respectively. The tortuosity of the crack pattern and the crack width is higher in TRC specimens subjected to monotonic loading compared to specimens subjected to fatigue loading.

The crack widths are computed from DIC for specimens subjected to both monotonic and fatigue loading using a line tool in the DIC Istra

4D software. The line is drawn across the crack at the bottom of the tension surface and the change in the length is measured in successive images. The load versus crack width obtained from monotonic loading and the number of load cycles versus crack width obtained from fatigue loading are superposed as shown in Figure 13. The crack width at failure under fatigue is about 0.13 mm which is significantly lower compared to the crack width at failure under monotonic loading (1.5 mm). Further, the crack width evolution trend under monotonic and fatigue loading are quite different. Under fatigue, the crack width increases linearly with fatigue load cycles until failure while the mid-point displacement depicts a non-linear trend (Figure 9). These results illustrate that there is no correlation between the crack length and crack width of TRC specimens tested under fatigue loading.

4 SUMMARY AND CONCLUSIONS

In this research, the behaviour of TRC under flexural fatigue loading is experimentally investigated. The TRC specimen is tested under a three-point bending configuration and the load-deflection response, stiffness degradation, and crack propagation are evaluated to understand the fatigue damage progression in TRC panels. Finally, a comparison is drawn between the monotonic and fatigue response of TRC panels. The important conclusions drawn from this research are:

1. The load-deflection response of TRC under fatigue shows sufficient loading carrying capacity until deflection corresponding to point M which lies at about 30 % of fatigue life. The fatigue

deflection corresponding to point M lies closer to the deflection corresponding to monotonic strain-hardening peak load. For the design purpose, the fatigue strength of TRC panels could be considered until 70 % of the deflection value corresponding to the strain-hardening peak load of monotonic response.

2. TRC panel under fatigue shows sufficient warning before failure, unlike plain concrete which fails suddenly. At the time of failure, textile reinforcement elongated and some of them got ruptured while a few of them were still

intact holding the specimen from falling. This feature of TRC will make it a good substitute for glass facades which shatters in severe cyclonic conditions in high-rise buildings.

3. The DIC analyses showed that the failure of TRC specimens due to fatigue loading takes place at a considerably lower crack width compared to the monotonic loading.

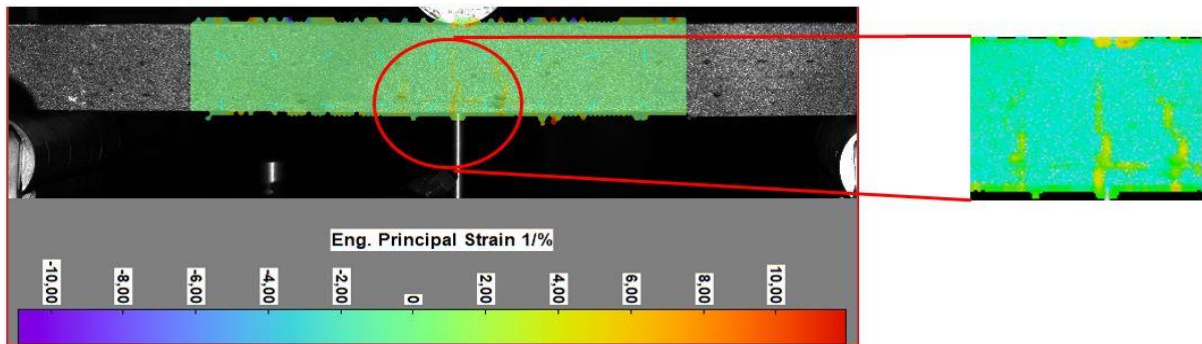


Figure 10: Crack propagation pattern under fatigue loading

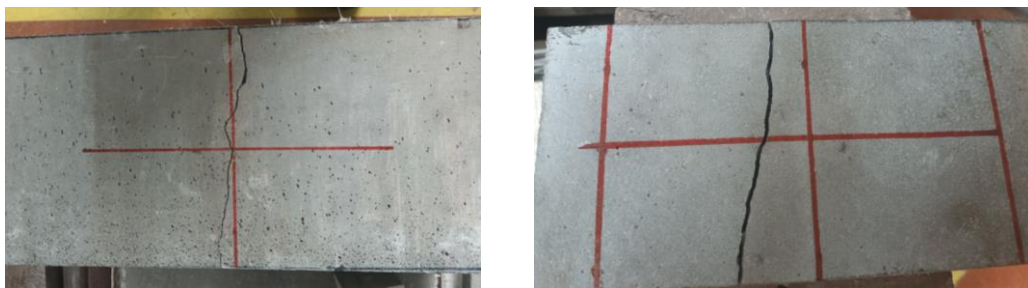


Figure 11: Crack pattern on the top face of TRC panel subjected to monotonic loading.

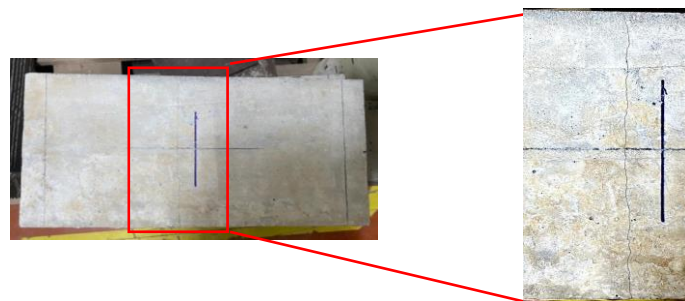


Figure 12: Crack pattern on the top face of TRC panel subjected to fatigue loading

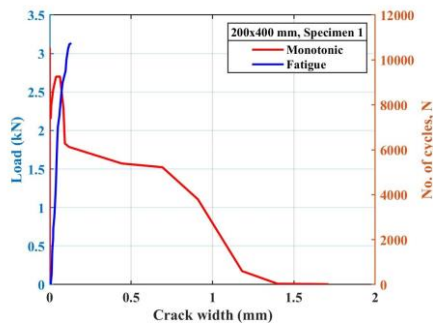


Figure 13: Comparison of crack width evolution in TRC panel subjected to monotonic and fatigue loading

5 ACKNOWLEDGEMENTS

The authors wish to thank the staff, researchers, and professors of the Building Technology and Construction Management (BTCM), Department of Civil Engineering, IITM, Chennai, India. The help of research scholars, Mr. Ramakrishna S and Mr. Sachin Paul is highly appreciated. The support through the Institute of Eminence Research Initiative Grant on Technologies for Low Carbon and Lean Construction (TLC2) from IIT Madras is acknowledged.

REFERENCES

- [1] Hegger, J., Schneider, M. and Kulas, C., 2010, September. Dimensioning of TRC with application to ventilated facade systems. In *International RILEM Conference on Material Science* (pp. 393-403). RILEM Publications SARL.
- [2] Williams Portal, N., Lundgren, K., Wallbaum, H. and Malaga, K., 2015. Sustainable potential of textile-reinforced concrete. *Journal of materials in civil engineering*, 27(7), p.04014207.
- [3] Laiblová, L., Vlach, T., Ženíšek, M., Řepka, J. and Hájek, P., 2018. Lightweight TRC facade panels with the LEDs. *Key Engineering Materials*, 760, pp.141-146.
- [4] Ahmed, M.A.A.E.D. and Fikry, M.A., 2019. Impact of glass facades on internal environment of buildings in hot arid zone. *Alexandria Engineering Journal*, 58(3), pp.1063-1075
- [5] Sahu, D., Kini, P., Kishore, P., Upadhyay, A. and Kamath, K., 2021. Impact of window wall ratio in office building envelopes on operational energy consumption in the temperate climatic zone of India. *Impact of window wall ratio in office building envelopes on operational energy consumption in the temperate climatic zone of India*. San Francisco, CA.
- [6] Klem, D., Farmer, C.J., Delacretaz, N., Gelb, Y. and Saenger, P.G., 2009. Architectural and landscape risk factors associated with bird–glass collisions in an urban environment. *The Wilson Journal of Ornithology*, 121(1), pp.126-134.
- [7] Hegger, J., Kulas, C. and Horstmann, M., 2011. Realization of TRC facades with impregnated AR-glass textiles. *Key Engineering Materials*, 466, pp.121-130.
- [8] Novotná, M., Kostecká, M., Hodková, J. and Vokáč, M., 2014. Use of textile reinforced concrete—especially for facade panels. *Advanced Materials Research*, 923, pp.142-145.
- [9] Papanicolaou, C.G., 2016. Applications of textile-reinforced concrete in the precast industry. In *Textile Fibre Composites in Civil Engineering* (pp. 227-244). Woodhead Publishing.
- [10] Vatin, N. and Korniyenko, S., 2022. Energy performance of buildings made of textile-reinforced concrete (TRC) sandwich panels. *Magazine of Civil Engineering*, 113(5), p.11303.
- [11] De Munck, M., Tysmans, T., Wastiels, J., Kapsalis, P., Vervloet, J., El Kadi, M. and Remy, O., 2019. Fatigue behaviour of textile reinforced cementitious composites and their application in sandwich elements. *Applied Sciences*, 9(7), p.1293.
- [12] Powar, O. and Jayachandran, A., 2021. Learning from Façade Failures over Urban

Landscape: Aftermath of Cyclone Vardah. *Natural Hazards Review*, 22(1), p.04020049.

[13] Brameshuber, W. ed., 2006. *Report 36: textile reinforced concrete-state-of-the-art report of RILEM TC 201-TRC* (Vol. 36). RILEM publications.

[14] Zhang, M. and Deng, M., 2022. Tensile behavior of textile-reinforced composites made of highly ductile fiber-reinforced concrete and carbon textiles. *Journal of Building Engineering*, 57, p.104824.

[15] Venigalla, S.G., Nabilah, A.B., Mohd Nasir, N.A., Safiee, N.A. and Abd Aziz, F.N.A., 2022. Textile-Reinforced Concrete as a Structural Member: A Review. *Buildings*, 12(4), p.474.

[16] Zargaran, M., Attari, N.K. and Alizadeh, S., 2023. Flexural behavior of high-performance and non-high-performance textile reinforced concrete composites. *European Journal of Environmental and Civil Engineering*, 27(2), pp.893-907.

[17] Hegger, J. and Voss, S., 2008. Investigations on the bearing behaviour and application potential of textile reinforced concrete. *Engineering structures*, 30(7), pp.2050-2056.

[18] Halvaei, M., Jamshidi, M., Latifi, M. and Ejtemaei, M., 2020. Experimental investigation and modelling of flexural properties of carbon textile reinforced concrete. *Construction and Building Materials*, 262, p.120877.

[19] Mesticou, Z., Bui, L., Junes, A. and Larbi, A.S., 2017. Experimental investigation of tensile fatigue behaviour of Textile-Reinforced Concrete (TRC): Effect of fatigue load and strain rate. *Composite Structures*, 160, pp.1136-1146.

[20] Wagner, J. and Curbach, M., 2019. Bond fatigue of TRC with epoxy impregnated carbon textiles. *Applied Sciences*, 9(10), p.1980.

[21] De Munck, M., Tysmans, T., Wastiels, J., Kapsalis, P., Vervloet, J., El Kadi, M. and Remy, O., 2019. Fatigue behaviour of textile reinforced cementitious composites and their application in sandwich elements. *Applied Sciences*, 9(7), p.1293.

[22] Shaker, K., Nawab, Y., Ayub Asghar, M., Nasreen, A. and Jabbar, M., 2020. Tailoring the properties of leno woven fabrics by varying the structure. *Mechanics of Advanced Materials and Structures*, 27(22), pp.1865-1872.

[23]<https://www.dantecdynamics.com/solution/digital-image-correlation-dic/>